OPEN

Correspondence and
requests for materials
should be addressed to
C.M. (monterolac@
ihpc.a-star.edu.sg)

Criticality of forcing directions on the fragmentation and resilience of grid networks

Cheryl Abundo[1,2], Christopher Monterola[1,3] & Erika Fille Legara[1,3]

[1]National Institute of Physics, University of the Philippines Diliman, Quezon City, Philippines 1101, [2]School of Physical and Mathematical Sciences, Nanyang Technological University 21 Nanyang Link, Singapore 637371, [3]Complex Systems Group, Institute of High Performance Computing, Computing Science, Agency for Science Technology and Research 1 Fusionopolis Way, Connexis (North Tower) Singapore 138632.

A general framework for probing the dynamic evolution of spatial networks comprised of nodes applying force amongst each other is presented. Aside from the already reported magnitude of forces and elongation thresholds, we show that preservation of links in a network is also crucially dependent on how nodes are connected and how edges are directed. We demonstrate that the time it takes for the networks to reach its equilibrium network structure follows a robust power law relationship consistent with Basquin's law with an exponent that can be tuned by changing only the force directions. Further, we illustrate that networks with different connection structures, node positions and edge directions have different Basquin's exponent which can be used to distinguish spatial directed networks from each other. Using an extensive waiting time simulation that spans up to over 16 orders of magnitude, we establish that the presence of memory combined with the scale-free bursty dynamics of edge breaking at the micro level leads to the evident macroscopic power law distribution of network lifetime.

T he emergence of complexity in various social, biological and physical systems is hinged upon the structure of the system and the interaction of its agents. To capture how systems change, it is necessary to understand how agents are connected and how links are formed and broken. In this study, we concentrate on the factors that drive the breakage of links in a network. We present a general framework for probing the dynamic evolution of spatial networks by considering the forces that nodes apply on each other along their links.

Upon reaching a critical amount of accumulated force, there are systems which experience sudden collapse. Road network links fail when vehicular congestion disrupts the flow of traffic[1,2]. Protein chains are driven far apart when large stresses are present between connected molecules[3]. But there are also some networks which exhibit a high degree of resilience to forcings. Communication networks can continue to transmit information even during partial router malfunctions[4]. Organisms reproduce and propagate even after efforts are made to halt their growth. Their unexpected tolerance to breaking forces has been attributed to their underlying network structure[5].

Several models have been developed to analyze the resilience of such networks to one time deletion of edges including random failures and targeted removals[5–7]. However, these models fail to capture the continuous dynamic breaking that is always at play in many networks. A network can initially demonstrate resilience but when continuously subjected to force, the accumulated damage can lead to network fragmentation or collapse. The distribution of forces in the network constantly changes every time an edge breaks and depending on how the edges are directed and how the nodes are connected, the final topology of the network may vary.

Here, we analyze the resilience of lattice networks with only short-range links, and those with both short and long-range links such as Erdos-Renyi (ER) and Barabasi-Albert (BA) networks by following their evolution as they continuously experience a constant amount of force among their nodes. We consider network types that are distributed in a spatial grid as widely seen in distributed parallel computing[4], router and sensor networks[4,7,8], distributed control manufacturing systems[4], satellite constellations[4], wired circuits[4], transport systems[1,2,9], electrical power grids[7–10] and protein chain networks[3]. In Supplementary Section S5 we present how any network spatial configuration can be embedded into a spatial grid and demonstrate this with an actual bus transport network (Supplementary Section S6).

Some of the factors that influence the disconnection of links in evolving networks are force magnitudes and duration of time these forces are applied. Here, we show that the robustness and tolerance of a spatial grid network

to edge failures is also contingent crucially on the direction of edges along which forces in the system are applied. Choosing the appropriate connection and direction patterns of the edges can optimize the distribution of load in the system and can consequently make a network more resilient to edge failures[7]. We consider two different edge direction patterns for the lattice, ER, and BA networks, (A) uniform force directions and (B) random force directions.

Results

Much of the work concerning network modelling do not incorporate the spatial positions of the nodes in the system. But as argued by Gastner *et al.*, nodes of real-world networks have well-defined positions that change over time, and incorporating spatial and temporal information into the analysis of networks give a better insight as to how a system behaves[1]. We consider lattice, ER, and BA networks embedded in Euclidean grid space[1] where the edges can either represent physical constructs or some abstract relationship.

Spatial grid network. Nodes with identical masses m are positioned in an $M \times N$ lattice labelled by (i, j) where $1 \leq i \leq M$ and $1 \leq j \leq N$ as illustrated in Fig. 1. Taking into consideration the ease of computation, the motion of each $(i, j)^{th}$ node is constrained to two dimensions $x_{i,j}$ and $y_{i,j}$. Each edge is an elastic simple Hookean spring with stiffness κ and unstretched length l_0. By virtue of being connected, two nodes experience a Hookean spring force proportional to the elongation of their edge $\Delta l \equiv l - l_0$ with κ being the constant of proportionality.

The nodes in the spatial grid can either be connected following the configuration of a lattice network (Fig. 1(a)–(b)), an ER network (Fig. 1(c)–(d)), or a BA network (Fig. 2). In the lattice network, connections are made using the Von Neumann neighborhood, forming $[(M - 1) \times N] + [M \times (N - 1)]$ connections. Moreover, free boundary conditions (FBC) are imposed. To keep the number of connections comparable across all networks considered, an approximately equivalent number of edges is formed for the ER and BA networks.

The directions of the edges represent the force directions in the grid network. The force directions in the network can either follow the uniform connection pattern shown in Fig. 1(a) and Fig. 1(c) or the random connection pattern shown in Fig. 1(b) and Fig. 1(d). For BA networks with uniform force directions, almost all edges were directed outward and all non-zero node in-degrees are only $k_{in} = 2$. On the other hand, for BA networks with random force directions, the number of edges directed outward is about the same as those directed inward as shown by their similar node in-degree and out-degree distributions in Fig. 2.

Force accumulation. Repeated application of force by the source or influential node to the target node, however small it may be, can eventually cause the failure of the edge linking them. Following the work of Carmona *et al.*[11], each edge is given a *memory* of its deformation history $\{\varepsilon(0), \varepsilon(\delta t), \varepsilon(2\delta t), \ldots, \varepsilon(t)\}$. At each time step, the elongation of the edge is computed and appended to the deformation history sequence. The edges have an infinite memory range which means that the *entire* deformation history is stored.

In determining whether a spring has broken or an edge has failed, we evaluate the *total damage* $q(t)$ of the spring as given by

$$q(t) = \varepsilon(t) + f_0 \sum_{t'=0}^{t'=t} \varepsilon(t'), \quad (1)$$

where $\varepsilon(t)$ is the instantaneous deformation and $f_0 \sum_{t'=0}^{t'=t} \varepsilon(t')$ is the accumulated damage due to repeated application of force[12,13]. An edge fails and the connection is broken when the *total damage* $q(t)$ of a specific edge exceeds the elongation threshold ε_{th} of that edge (Supplementary Fig. S1). In the absence of memory, $\varepsilon(t)$ dominates and a network only fragments for force magnitudes above the limit. Accounting for memory allows subcritical loading where cyclical application of force causes progressive edge failures leading to a substantial fraction of edges to break. The contribution of the immediate deformation and the memory of accumulated damage is controlled by the parameter f_0 which we choose to be 0.05 for this study.
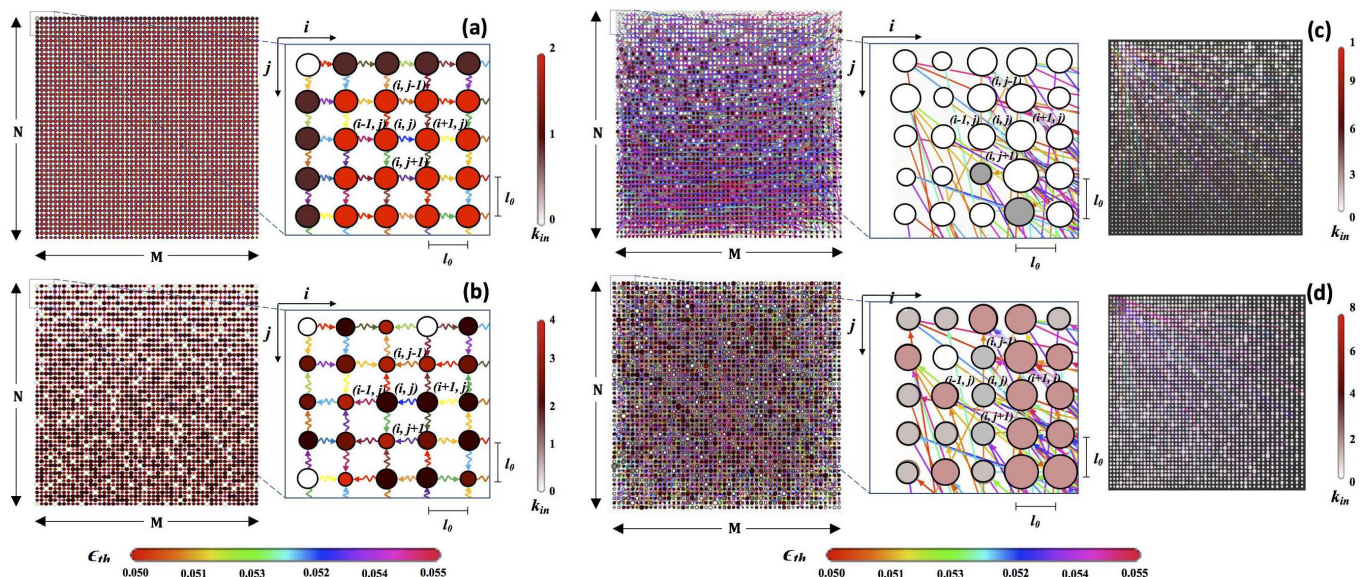

Figure 1 | Network architecture and index conventions. (a) represents a lattice network with uniform force directions and (b) random force directions. In (c) and (d) nodes are arranged spatially in a grid and $[(M - 1) \times N] + [M \times (N - 1)]$ edges are randomly chosen from possible connections. (c) represents an ER network where forces are directed with the highest level of uniformity and (d) randomly. Edge colors correspond to the elongation thresholds ϵ_{th} while node colors are based on the degree of incoming connections k_{in}. Node sizes correspond to the degree of outgoing connections k_{out} (largest node has higher k_{out}). Arrows are directed from source to target node. Figures in the last column highlight the edges of the shown selected nodes.
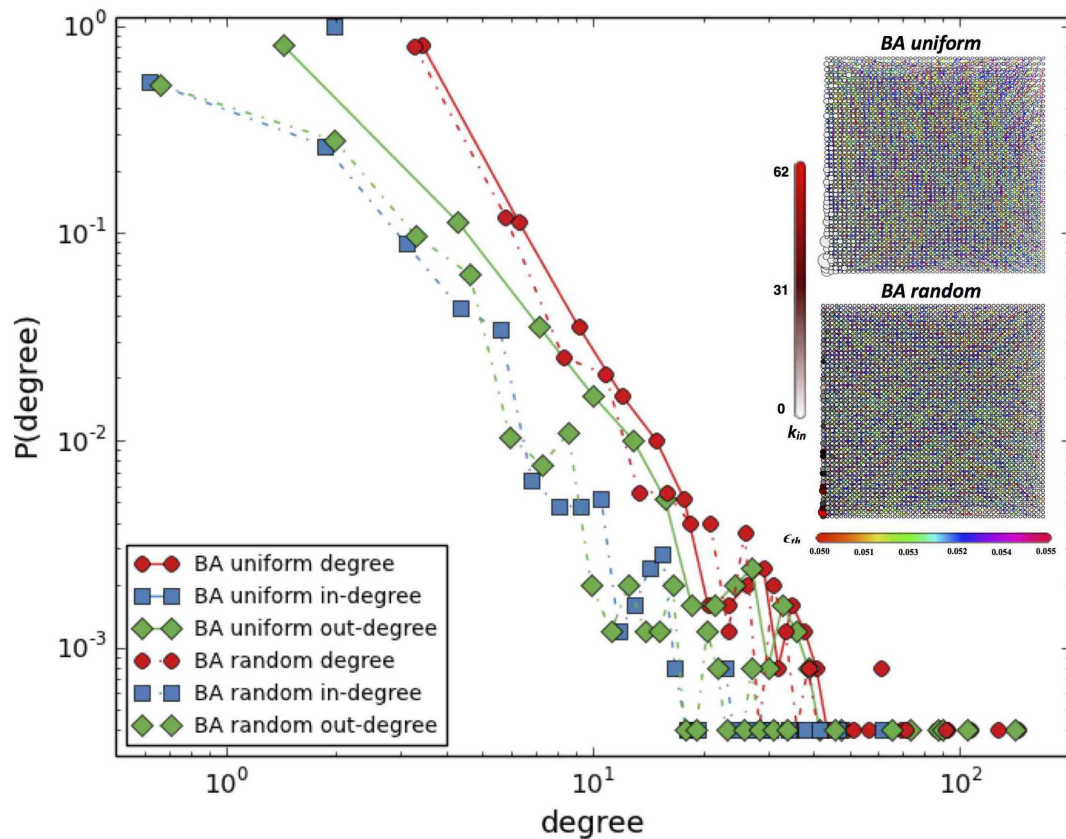
Figure 2 | Network architecture and degree distribution of Barabasi-Albert networks with uniform and random force directions. Almost all edges were directed outward for the uniform case while comparable number of edges were directed inward and outward for the random case. In the inset, nodes are sized according to k_{out}.

At this value of f_0, the disorder in the fragmentation process is controlled and the effects of the interfering elastic waves are eliminated[13]. Choosing a smaller f_0 only lengthens all fragmentation processes and does not change any of our results.

Breaking dynamics. At the onset of the simulation, all nodes are at rest and located at their initial positions. The time evolution of the grid network is followed by solving the equations of motion of each of the nodes using an iterative fourth order Runge-Kutta method. As shown in the work of Esleta *et al.*, a time step of $\delta t = 2^{-10}$ produces $\delta\xi \sim 9 \times 10^{-4}$ total accumulated global error which causes no significant position and velocity errors (see Supplementary Section S2)[12]. The equations of motion is a set of second-order coupled differential equations given by

$$m\ddot{\vec{r}}_{(i,j)} = \vec{F}_{(i,j)}, \qquad (2)$$

where $r_{(i,j)} \equiv x_{(i,j)}\hat{e}_x + y_{(i,j)}\hat{e}_y$ is the displacement of mass (i,j) from its initial position in the grid[12]. The total force $\vec{F}_{(i,j)} \equiv F^x_{(i,j)}\hat{e}_x + F^y_{(i,j)}\hat{e}_y$ acting on mass (i,j) is a combination of the applied force $\vec{F}_{app}$ and interparticle forces

$$\vec{F}_{(i,j)} \equiv \vec{F}_{app} + \vec{f}_{(i,j+1)-(i,j)} + \vec{f}_{(i-1,j)-(i,j)} + \vec{f}_{(i+1,j)-(i,j)} + \vec{f}_{(i,j-1)-(i,j)}. (3)$$

Force is applied between connected nodes and has the same magnitude for all edges. The directions of the applied forces $\left\{F^k_{app}\right\}$ were either (A) uniform or (B) random. In method A, the directions of F_{app} were made to have the highest degree of uniformity (Supplementary Fig. S3, Fig. S5 and Fig. S7). In method B, we scan all

edges of the grid network at the start of the simulation, and for each edge, we choose a node randomly and assign this node as the target node (Supplementary Fig. S4, Fig. S6 and Fig. S8). The applied force is then directed from source to target node. Doing so, allows us to explore whether the final fragmented structure of the grid network is affected by the direction of F_{app}. Each network simulation was run for at least three realizations.

The interparticle forces acting on node (i,j) is solved by computing for the deformation vector $\vec{\varepsilon}_{(i\pm1,j\pm1)-(i,j)}$ of its edges[12]. From the geometry of the system as shown in Supplementary Fig. S2, the horizontal deformations are

$$\varepsilon^x_{(i,j+1)-(i,j)} = \left[1 - \frac{l_0}{\sqrt{\left(x_{i,j}-x_{i,j+1}\right)^2 + \left(y_{i,j}-y_{i,j+1}-l_0\right)^2}}\right]\left(x_{i,j}-x_{i,j+1}\right)$$

$$\varepsilon^x_{(i-1,j)-(i,j)} = \left[1 - \frac{l_0}{\sqrt{\left(x_{i,j}-x_{i-1,j}+l_0\right)^2 + \left(y_{i,j}-y_{i-1,j}\right)^2}}\right]\left(x_{i,j}-x_{i-1,j}+l_0\right)$$

$$\varepsilon^x_{(i+1,j)-(i,j)} = \left[1 - \frac{l_0}{\sqrt{\left(x_{i,j}-x_{i+1,j}-l_0\right)^2 + \left(y_{i,j}-y_{i+1,j}\right)^2}}\right]\left(x_{i,j}-x_{i+1,j}-l_0\right)$$

$$(4)$$

$$\varepsilon^x_{(i,j-1)-(i,j)} = \left[1 - \frac{l_0}{\sqrt{\left(x_{i,j}-x_{i,j-1}\right)^2 + \left(y_{i,j}-y_{i,j-1}+l_0\right)^2}}\right]\left(x_{i,j}-x_{i,j-1}\right),$$

while the vertical deformations are

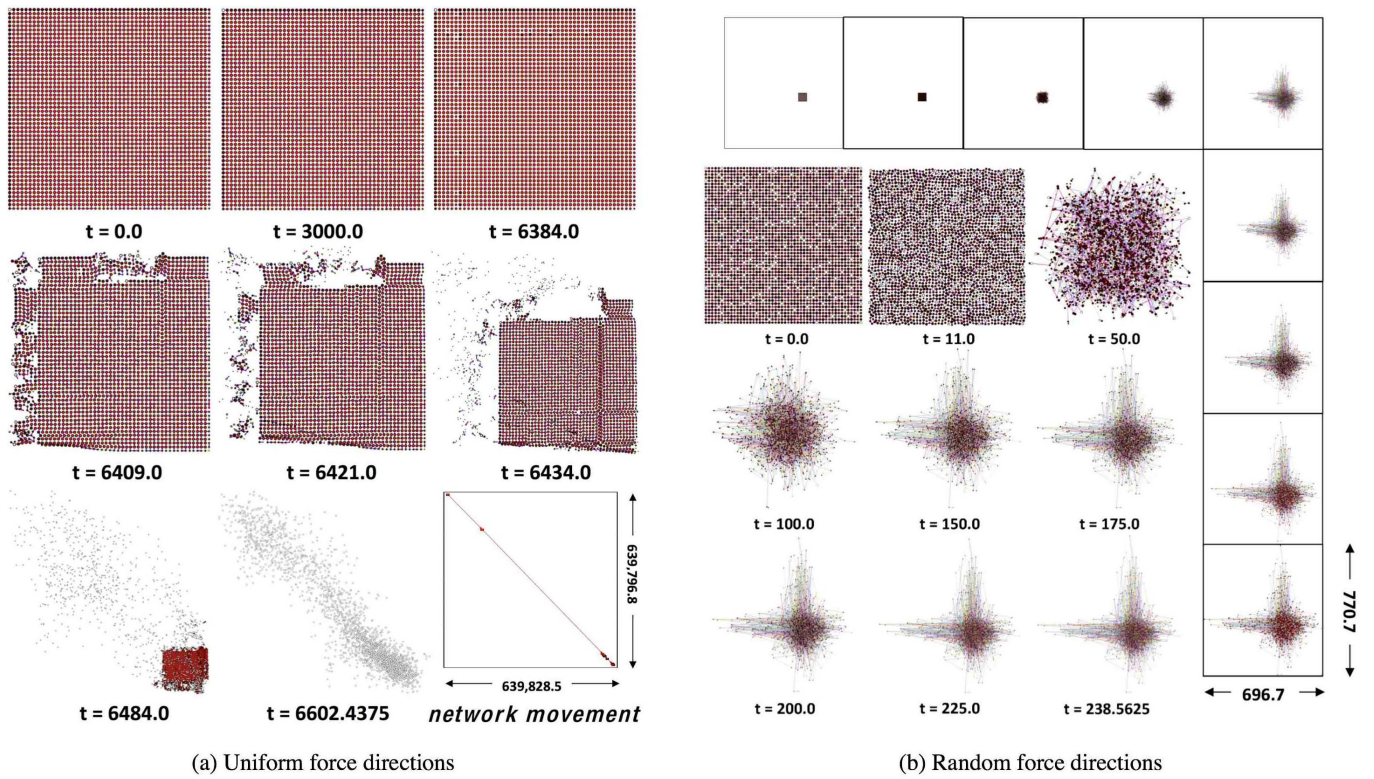(a) Uniform force directions

(b) Random force directions

Figure 3 | Evolution of a lattice network. (a) For uniform force directions and $F_{app} = 0.03$, breaking starts near the top and left sides at $t = 6{,}384.0$. Failure cascades and last to be disconnected are edges near the bottom right corner where the least amount of force is felt. The network totally collapses at $t = 6{,}602.4$. No connections remain and the network elongates and moves diagonally following the net force. (b) For random force directions and $F_{app} = 0.03$, breaking starts at $t = 11.0$ at random positions. The network reaches its equilibrium structure at $t = 238.6$ with only 0.496 ± 0.007 of the edges disconnected.

$$\varepsilon^y_{(i,j+1)-(i,j)} = \left[1 - \frac{l_0}{\sqrt{\left(x_{i,j}-x_{i,j+1}\right)^2 + \left(y_{i,j}-y_{i,j+1}-l_0\right)^2}}\right]\left(y_{i,j}-y_{i,j+1}-l_0\right)$$

$$\varepsilon^y_{(i-1,j)-(i,j)} = \left[1 - \frac{l_0}{\sqrt{\left(x_{i,j}-x_{i-1,j}+l_0\right)^2 + \left(y_{i,j}-y_{i-1,j}\right)^2}}\right]\left(y_{i,j}-y_{i-1,y}\right)$$

$$\varepsilon^y_{(i,j-1)-(i,j)} = \left[1 - \frac{l_0}{\sqrt{\left(x_{i,j}-x_{i,j-1}\right)^2 + \left(y_{i,j}-y_{i,j-1}+l_0\right)^2}}\right]\left(y_{i,j}-y_{i,j-1}+l_0\right) \quad (5)$$

$$\varepsilon^y_{(i+1,j)-(i,j)} = \left[1 - \frac{l_0}{\sqrt{\left(x_{i,j}-x_{i+1,j}-l_0\right)^2 + \left(y_{i,j}-y_{i+1,j}\right)^2}}\right]\left(y_{i,j}-y_{i+1,j}\right).$$

The edges are assumed to be Hookean springs and as such the interparticle force is $\vec{f}_{(i\pm1,j\pm1)-(i,j)} = -\kappa\vec{\varepsilon}_{(i\pm1,j\pm1)-(i,j)}$. Using the deformations given by equations 4 and 5 to derive the interparticle forces exerted by the springs and combining them with $\vec{F}_{app}$, the horizontal component of the total force $\vec{F}_{i,j}$ acting on (i,j) is

$$F^x_{i,j} = F^x_{app} + \kappa\left[\varepsilon^x_{(i,j+1)-(i,j)} - \varepsilon^x_{(i-1,j)-(i,j)} + \varepsilon^x_{(i+1,j)-(i,j)} - \varepsilon^x_{(i,j-1)-(i,j)}\right], (6)$$

while the vertical component is

$$F^y_{i,j} = F^y_{app} + \kappa\left[\varepsilon^y_{(i,j+1)-(i,j)} - \varepsilon^y_{(i-1,j)-(i,j)} - \varepsilon^y_{(i,j-1)-(i,j)} + \varepsilon^y_{(i+1,j)-(i,j)}\right], (7)$$

After solving for the displacement of each node in the grid network, the condition for breaking is evaluated for all intact edges. Although the equation of motion considered does not include a velocity-dependent term, the networks studied still take this into account by considering the entire history of deformations which together with the instantaneous force can cause a link to break. If the elongation of the spring exceeds ε_{th}, the edge is removed from further calculations. The elastic energy of the broken link is released and redistributed to the edges of its nearest connected nodes[12]. The breakage of a particular link causes cascading disconnections and may eventually lead to network collapse.

Results for lattice network. The spatial arrangement of nodes in a network affects the distribution of force in the system and dictates the degree of influence a node has as compared to other nodes. In some cases, direct interactions among components are only possible between spatial neighbors. We analyze this configuration using a 50×50 lattice network with 4,900 edges.

Uniform force directions. The forces in a system can be directed uniformly such that all vertical and horizontal F_{app} have the same directions. This results to a net force directed diagonally in the network. Such forcing pattern also allows nodes to be influenced only by nodes that are to their right and below them (see Supplementary Section S3.A.1).

As the network evolves, a cascading disconnection of edges is observed as shown in Fig. 3(a). The first to break are the edges near the top and left sides since they feel the greatest amount of force. The edges' disconnection pattern follows the direction of the net force which is diagonally towards the most influential node at the bottom right corner. This node-to-node forcing pattern results to a global acceleration that causes the network to elongate diagonally towards the bottom right corner as shown in the network movement of Fig. 3(a). Directing all forces towards the most influential node will globally affect the entire network to move towards the direction of this node.
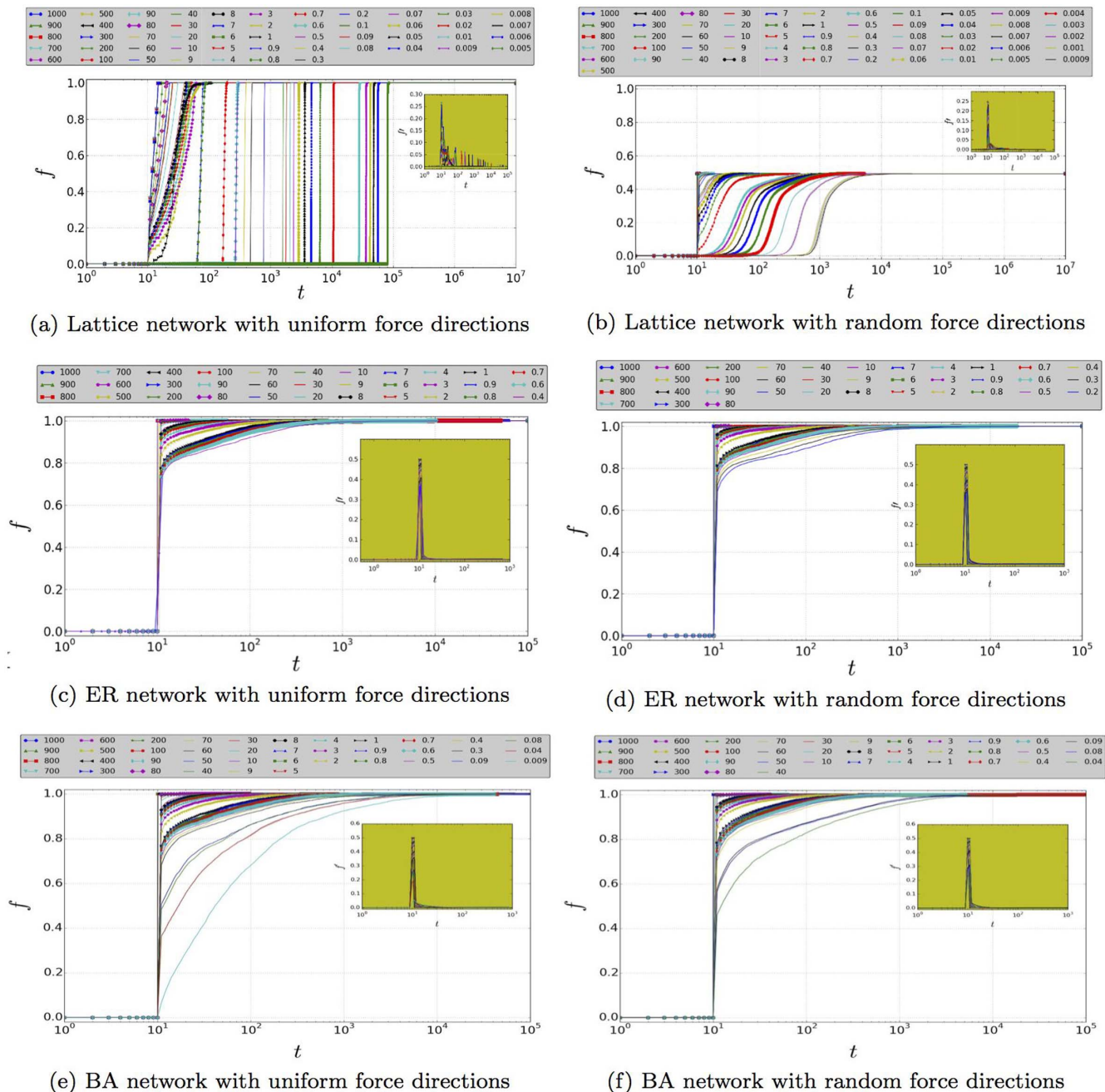
(a) Lattice network with uniform force directions

(b) Lattice network with random force directions

(c) ER network with uniform force directions

(d) ER network with random force directions

(e) BA network with uniform force directions

(f) BA network with random force directions

Figure 4 | Fraction of disconnected edges f in grid networks. (a) Lattice networks with uniform force directions totally collapse while for those with (b) random force directions, 0.503 ± 0.006 of the edges disconnects. (c–d) Regardless of the magnitude and directions of $\{F_{app}\}$, an ER network experiences total system collapse. (e–f) BA networks completely fragment regardless of the magnitude and directions of $\{F_{app}\}$. The insets show the derivative of f or the disconnection rate of the edges. The rate of disconnection f' at the transition point decreases with F_{app} in all networks. For lattice networks, randomizing force directions further decreased the rate of disconnections.

Fig. 4(a) shows the fraction of disconnected edges f as a function of time for all values of applied forces used when the direction of F_{app} in the network is uniform. The behavior of f follows a threshold function similar to an inverse bond percolation model. We find that edges started to fail at different times depending on the F_{app} used. The smaller the magnitude of force applied by the nodes, the longer the agents stay in the network.

An abrupt change in the network's state is observed after a small additional force is applied[8]. The lattice network failure observed here does not gradually become more likely but instead there is a transition point during which disconnections are fastest as shown by the disconnection derivative f' in the inset of Fig. 4(a). Around this critical point, any additonal force causes a sizeable amount of edges

to fail, eventually leading to a complete network collapse. But decreasing F_{app} can help slow down the disconnections.

Random force directions. The directions of the applied forces in a lattice network are random when the influential nodes of the network are positioned randomly in grid space. Some nodes are influenced by only a few nodes while others receive much influence (see Supplementary Section S3.A.2). The directions of $\left\{F_{app}^k\right\}$ are assigned at the start of each simulation and are maintained constant. Initial breakings start at random positions in the lattice as shown in Fig. 3(b). As a result of assigning this directionality of interactions, the nodes disperse away from the initial center of the network with more nodes
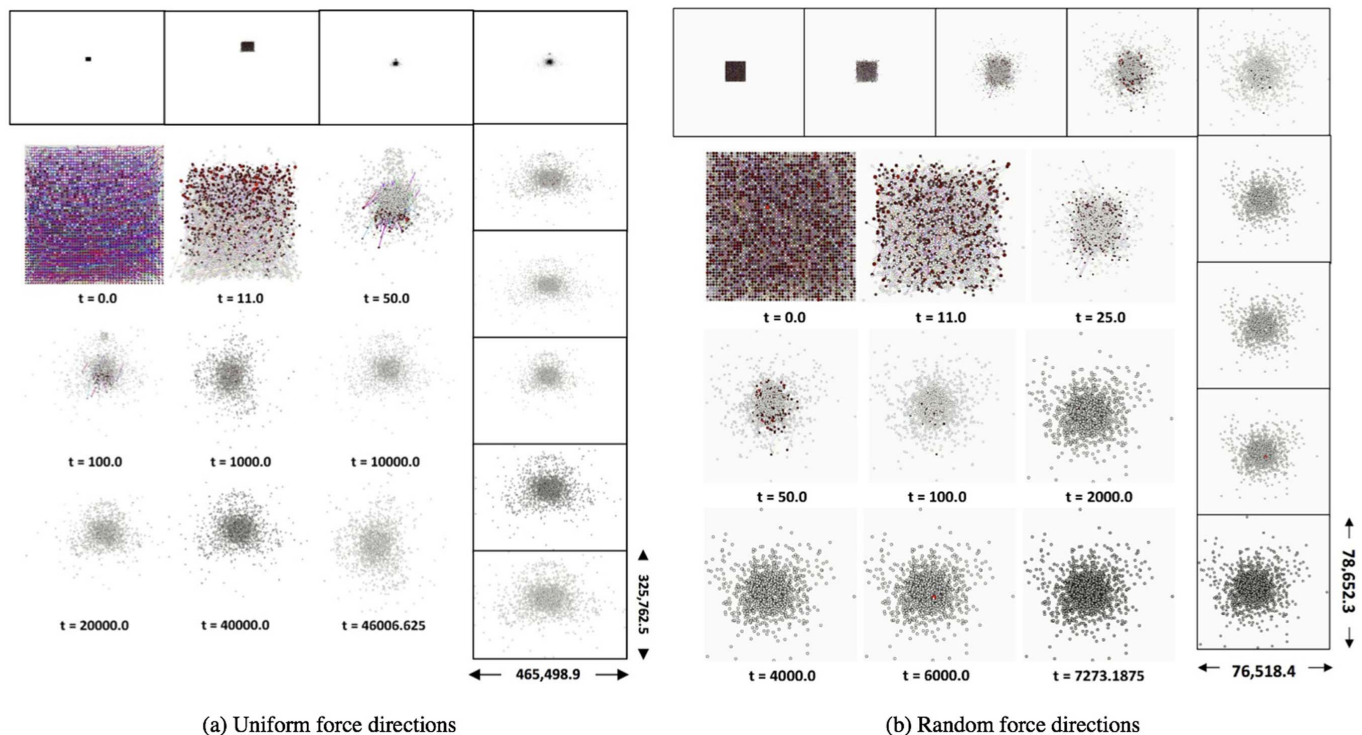
(a) Uniform force directions

(b) Random force directions

Figure 5 | Evolution of an Erdos-Renyi network. (a) For uniform force directions and $F_{app} = 0.8$, breaking starts with nodes disconnecting from the influential nodes at the bottom resulting to 77.6% of the edges to break instantly. By $t = 100$, 95.7% of the edges have disconnected. The remaining edges take far longer to disconnect. (b) For random force directions, breaking starts at random positions. Initial disconnections account for 79.6% of the edges. By $t = 100.0$, 97.0% of edges have disconnected. The remaining 3.0% breaks slower until the network completely collapses at $t = 7,273.2$.

moving upward and to the left. This bias towards the upward and right directions is a result of the randomization which positions 68 (2.72%) more influential nodes to the right and 34 (1.36%) more influential nodes at the top. But this net drift is only 0.11% of the drift when forcings are uniform. The random placement of the influential nodes in the network aids in preserving some of the connections in the network and prevents large magnitude changes in the global position of the network.

The preservation of links is reflected in Fig. 4(b) which shows the fraction of disconnected edges f as a function of time for all values of applied forces. Similar to lattice networks with uniform force directions, the failure of the edges has a characteristic phase transition. But we find that randomizing the force directions in a lattice network results to a more resilient network. For all F_{app}, lattice networks of this type preserve more than half of its edges with only 0.496 ± 0.007 disconnected edges.

Results for Erdos-Renyi network. Examining the evolution of a random network or an ER network remains significant even after real-world networks were found to be otherwise. Systems like the power grid or the neural network of *C.elegans* are best described as evolving networks[14]. The development of such evolving networks are characterized by not only a power-law but also by exponential degree distributions[14]. Preferential attachment, aging effects and constraints in the growth of a network can in the long run lead to a transition to an exponentially decaying degree distribution. It is in this regime of the dynamic evolution of a network that findings regarding the resilience of an ER network may be of importance.

Uniform force directions. Though connections among nodes in an ER network are random, forcing directions can be made as uniform as possible by preferring specific positions in placing influential nodes (i.e. bias in vertical interactions such that nodes are influenced only by those below them) as discussed in Supplementary Section S3.B.1.

The first disconnections are the result of nodes breaking away from the more influential nodes at the bottom as illustrated in Fig. 5(a). Being influential allows an agent to affect more nodes but this can also mean that their connections are more likely to be short-lived. A cascade of disconnections from the more influential nodes is observed at just a short period of time. But there are some connections that persist far longer than others. As the network evolves, the individual node-to-node force interactions lead to a more dispersed network with the nodes moving outward with a slight drift downwards towards the influential nodes.

Random force directions. In randomizing the force directions in an ER network, we are distributing the influentials in grid space. For such case, nodes are influenced by other nodes regardless of their position (see Supplementary Section S3.B.2). Since influence is distributed, there is no bias in the global movement of the network and breaking also starts in random positions as shown in Fig. 5(b). Similar to the uniform force directions case, a large amount of edges fail initially (79.6% of edges). In a span of 100 iterations, 97.0% of the edges have already failed. The remaining 3.0% of the edges persists longer and disconnections slow down until the network totally collapses. Randomizing force directions also leads to a one order of magnitude decrease in the global dispersion of the nodes from the center of the network.

Results for Barabasi-Albert network. Most real world networks from cellular and genetic networks to social, citation, infrastructure and transport networks exhibit scale-free degree distributions that is well represented by BA networks[14,16–18]. We investigate here how the direction of forces affect the fragmentation of networks having scale-free degree distributions.

Uniform force directions. One of the key attributes of BA networks is the presence of a hub responsible for most of the connections in the network. In the uniform force directions case shown here, most of the
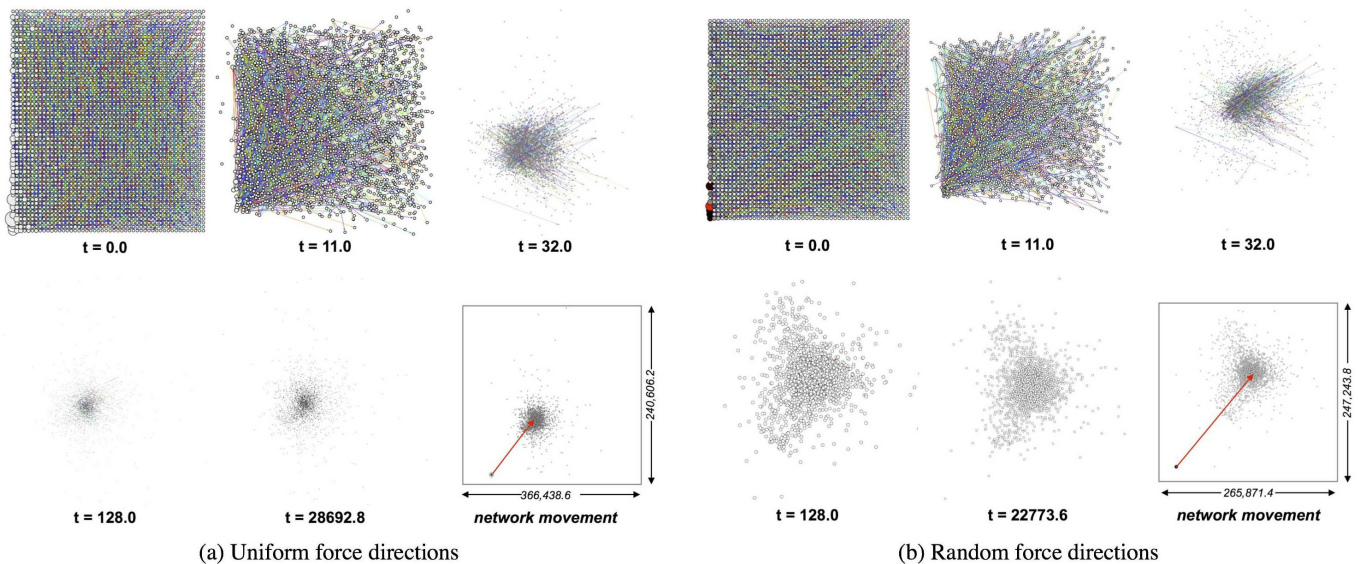
(a) Uniform force directions

(b) Random force directions

Figure 6 | Evolution of a Barabasi-Albert network. (a) For uniform force directions and $F_{app} = 0.8$, 75.9% of the edges fail instantly and by $t = 128.0$, 96.7% of the edges has disconnected. The remaining edges have all disconnected by $t = 28,692.8$. (b) For random force directions and $F_{app} = 0.8$, 75.9% of the edges fail instantly with only 1.9% of the edges remaining by $t = 128.0$. The network completely fragments at $t = 22,773.6$.

edges are directed away from the hub while all others are connected by preferring a certain direction as further illustrated in Supplementary Section S3.C.1. Another uniform directions case where edges are directed towards the hub (Supplementary Section S4) was also considered and found to have similar results.

Since the hub contains most of the connections and controls the movement of most nodes, the network eventually becomes completely fragmented but 3.3% of the edges take far longer to disconnect as shown in Fig. 6(a). The hub, being connected to a large number of nodes scattered throughout the spatial grid network, is pulled in all directions triggering a cascade of disconnections until no connection remains in the network regardless of F_{app} as shown in Fig. 4(e). Connections to nodes farthest to the hub are the first ones to break and are left far in space from the cluster of nodes as depicted in the network movement in Fig. 6(a).

Random force directions. Randomizing force directions meant keeping the number of hub edges that are directed inward and outward comparable. This allowed nodes other than the hubs to have paths to almost all nodes as discussed in Supplementary Section S3.C.2. However, the presence of a hub still led to complete network fragmentation as shown in Fig. 4(f).
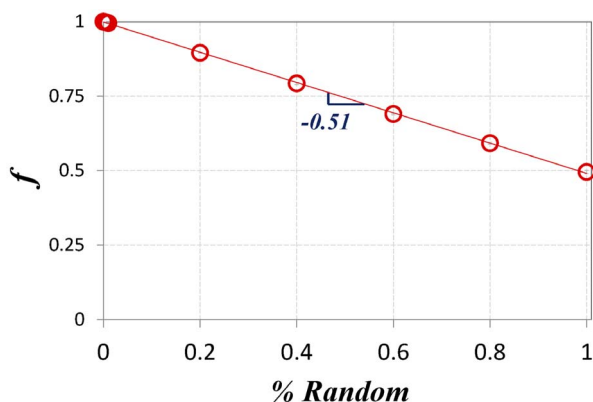

Figure 7 | The final fraction of disconnected edges in a lattice network with varying degree of force directions randomness. The relationship is found to be linear with a slope of −0.51.

Redistribution of forces and addition of paths among the network nodes were not enough to overcome the influence of the hubs. This holds regardless of the position of the hubs in grid space (Supplementary Section S4). Although preservation of connections was not achieved by randomizing force directions, nodes in this case are spatially closer. Random force directions kept the nodes closer by 34.1% in terms of area.

In Supplementary Section S6 we discussed in detail how the framework here can be applied to an actual bus transport network.

Dependence of the preservation of links on the randomness of the force directions. We have so far explored networks with force directions that are either completely uniform or completely random. We further examine the effect of the force pattern by combining uniform and random force directions in the lattice network. A fraction p of the edges had force directions that were randomized while the remaining edges experienced forces that had the same vertical and horizontal directions.

From Fig. 7, the fraction of disconnected edges in the final network is seen to follow a linear relationship with a slope of −0.51. The lattice network contains more disconnected edges as the force directions become more random. With the introduction of increased randomization, forces in the network become less concentrated causing edge failures to be more spatially distributed. This suggests that a force pattern that is most dissimilar to the connectivity pattern of the network may be the most ideal in constructing a resilient network. In the lattice network, nodes are connected uniformly such that only nearest neighbor connections are allowed. Subsequently, completely random force directions prove to be the best choice in preventing significant network fragmentation.

This provides an explanation as to why the final number of edges in the ER and BA networks were not found to depend on force directions. Since both long-range and short-range links are allowed and edges can be of varying spatial angle, the uniform force directions case is not of totally uniform edge directions. This results to the presence of some degree of randomization even in the uniform force directions pattern case.

Lifetime of Grid Network. Fig. 8(a) shows the lifetime of the networks as a function of F_{app}. The evolution of all the networks considered with deformation memory follows *Basquin's Law* at the regime below the force limit, F_{limit}, with lifetimes having a power law

7

(a) Lifetime of grid network
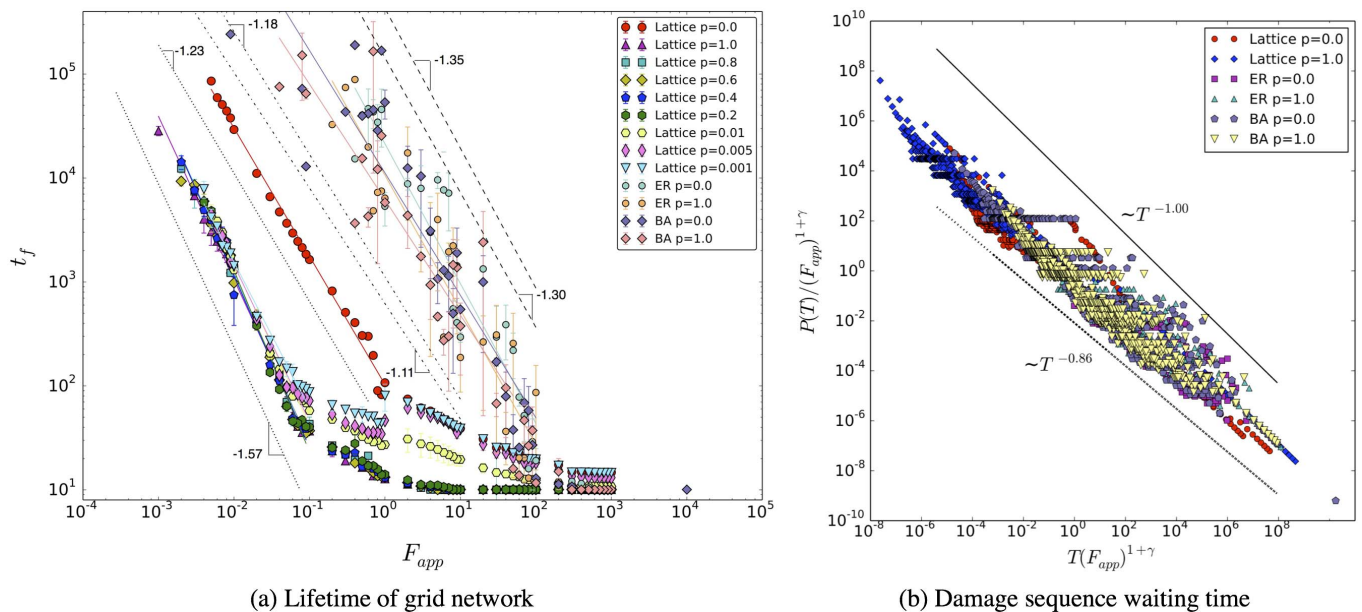
(b) Damage sequence waiting time

Figure 8 | Lifetime of grid networks. Dashed lines in (a) are to illustrate the *Basquin's exponent* of the networks. (b) shows that the macro-scale network lifetime results from microscopic scale-free waiting times between bursts. The lines shown are the range of exponents of the power-law distribution.

behavior with respect to F_{app}. When $F_{app} > F_{limit}$, instantaneous breakings dominate causing t_f to deviate from a power law behavior[11]. F_{limit} is approximated by setting $f_0 = 0$ and looking for the force magnitude for which (1) no fragmentation occurs for 5,000,000 iterations (at least one order of magnitude above the lifetimes of the networks considered), and (2) t_f decays rapidly with increasing F_{app}[13]. For lattice networks with uniform force directions, $F_{limit} = 1.21$ while for the case with a fraction of random force directions, F_{limit} is smaller at 0.09 ± 0.03. The ER networks followed *Basquin's Law* at forces below 103 for both cases. F_{limit} of the BA networks, on the other hand, is 111 for the uniform force directions case and 55 for the random force directions case.

In the work of *Carmona et al.*[11], they showed that it's possible to change the *Basquin's exponent*, γ, up to a magnitude of 0.40 by using different breaking thresholds. Using the same method they employed in calculating for *Basquin's exponent*, we demonstrate that γ, even for the same breaking rules, can be tuned by either altering (1) the network structure or (2) the force directions pattern.

For the same lattice network, a change in γ of magnitude 0.31 was achieved by randomizing the force directions of even only 0.1 of the links. For the ER networks, a minimal change of 0.05 in γ was found, providing added evidence that the uniform force directions method was not successful in "regularizing" the structure of the random network. A small change of 0.07 in γ was also found for BA networks. The presence of both long-range and short-range links in the ER and BA networks causes a minimal change in the characteristic exponent of their lifetimes when force directions are changed. In both networks, however, the random force directions case had a smaller γ magnitude which implies that on average, network fragmentation can be delayed by randomizing force directions.

The fragmentation process proceeds in bursts with a universal scale-free distribution. The bursty dynamics of edge breaking in the micro-level when memory is incorporated leads to the macro-scale power law distribution of network lifetime[11,15]. We illustrate this in Fig. 8(b) where the waiting time T between breakings has a power-law distribution $P(T)$ and $<T> \sim (F_{app})^{-(1+\gamma)}$. Having networks of very different degree distributions all demonstrating the same feature hints to the universality of this evolutionary dynamics and scale-free network lifetime.

Discussion

Modelling the evolution of a network through time as a result of the interplay of forces within the network and embedding the network in Eucledian space can provide a more realistic view of how network topology and structure change. Here, we investigate the eventual network structure of a directed spatial grid network with lattice, ER, or BA connections as a result of the forces that the nodes apply on each other along the edges linking them. The method presented here is general and can be used to probe other kinds of spatial networks as illustrated in Supplementary Section S5.

For a lattice network, uniform edge directions which result to force influence of nodes to systematically increase in spatial grid lead to an inevitable network collapse for all values of F_{app} in a network having a memory factor of 0.05. Such edge directions pattern results to the maximum amount of force to be applied to nodes of lesser force influence (i.e. nodes with no outgoing edges and hence do not apply force on any node) leading to a network of completely non-interacting components. But randomly positioning the influential nodes (i.e. nodes with more outgoing edges than incoming edges) results to a more distributed force which helps in preserving network relationships and keeps the giant cluster intact as shown in Supplementary Fig. S18 and Fig. S19. A lattice network is hence more resilient when the force sources are distributed randomly in the network instead of uniformly arranging them.

However in the same lattice network, when forces are uniformly directed, the start of breaking happens at a later time (Supplementary Fig. S18), at which point, nodes have already moved far from their initial positions. But as seen in the rate of disconnections, once breaking has begun, transitions are slower for networks with random force directions. This is true for all values of applied force which shows that the final topological and connection configuration of a lattice network is dependent on the force directions, but not on the magnitude of applied forces.

For an ER network, the transition to its fragmented state is seen to be faster than in a lattice network (Supplementary Fig. S18). The magnitude of F_{app} also fails to extend the start of network collapse unlike in lattice networks wherein lowering the magnitude of the applied force makes the network intact for longer periods of time. Here, a significant amount of the edges (0.79 ± 0.12) disconnects and the size of the largest cluster suddenly drops at the early part of the

simulation (Supplementary Fig. S20) for all the force magnitudes considered. On the other hand, for edges with higher thresholds, decreasing F_{app} can help extend their lifetime.

The final composition of an ER network is also found to be independent of the force directions. For both the uniform and random forcing direction cases, no edge or link between any node is preserved. If we base the resilience of an ER network on its final topological state, no improvement in the network's resilience can be achieved by changing the interconnection pattern of the network unlike that observed in the lattice network.

Similar to the ER network, a BA network also completely fragments regardless of force directions. This results from the presence of hubs responsible for most of the connections in the network and thereby causing forces to be more concentrated. When looking at the fraction of disconnected edges (Fig. 4) and the number of clusters (Supplementary Fig. S18), the BA network exhibits the same behavior as an ER network primarily because both contain a combination of long-range and short-range links. However, examining the size of the largest component reveals that the presence of hubs as in a BA network (Supplementary Fig. S21) slows down the fragmentation of the largest cluster in the early stages of fast breakings as compared to an ER network (Supplementary Fig. S20).

Decreasing the magnitude of forces slows down fragmentation regardless of network structure, but is only successful in delaying the onset of fragmentation in lattice networks. For lattice networks, an increase in the randomization of force directions can further lead to a decrease in the rate of fragmentation. Changing the direction of forces has no effect in the rate of fragmentation for both ER and BA networks providing an indication as to why their final state were the same regardless of force directions.

The lifetimes of the networks defined as the amount of time it takes for the network to reach its equilibrium f are also found to have a power law behavior following Basquin's Law. We further extend the work of *Carmona et al.*[11] by demonstrating that *Basquin's exponent,* γ, can be altered by changing only the force directions in the network without altering the network breaking thresholds. By looking at the waiting time between successive edge failures, we found that in the presence of deformation memory, the failure process proceeds in bursts with a universal scale-free distribution. This micro-scale bursty breaking of edges leads to the macro-scale power law distribution of network lifetime. This holds true for networks of very different degree distributions hinting to the universality of this mechanism.

1. Gastner, M. & Newman, M. The spatial structure of networks. *Eur. Phys. J. B* **49**, 247–252 (2006).
2. Yamins, D. & Rasmussen, S. Growing urban roads. *Networks and Spatial Economics* **3**, 69–85 (2003).
3. Ringler, P. & Schulz, D. Self-assembly of proteins into designed networks. *Science* **302**, 106–109 (2003).
4. Barrenetxea, G., Beferull-Lozano, B. & Vetterli, M. Lattice networks: capacity limits, optimal routing, and queueing behavior. *IEEE/ACM Trans. Netw.* **14**, 492–505 (2006).
5. Albert, R., Jeong, H. & Barabasi, A. L. Error and attack tolerance of complex networks. *Nature* **406**, 378–382 (2000).
6. Cohen, R., Erez, K., ben Avraham, D. & Havlin, S. Breakdown of the Internet under Intentional Attacks. *Phys. Rev. Lett.* **86**, 3682–3685 (2001).
7. Callaway, D., Newman, M., Strogatz, S. & Watts, D. Network robustness and fragility: percolation on random graphs. *Phys. Rev. Letters* **85**, 5468–5471 (2000).
8. De Marco, C. A phase transition model for cascading network failure. *Control Sys. Mag.* **21**, 40–51 (2001).
9. Wang, J. & Rong, L. Edge-based-attack induced cascading failures on scale-free networks. *Physica A* **388**, 1731–1737 (2009).
10. Nedic, D., Dobson, I., Kirschen, D., Carreras, B. & Lynch, V. Criticality in a cascading failure blackout model. *Int. J. of Electrical Power and Energy Sys* **28**, 627–633 (2006).
11. Carmona, H. A., Kun, F., Andrade, J. S. Jr. & Herrmann, H. J. Computer simulation of fatigue under diametrical compression. *Phys. Rev. E* **75**, 046115 (2007).
12. Esleta, G. A. & Monterola, C. Structural reinforcement in a spring-block model of stress-induced fracture propagation. *Comput. Phys. Commun.* **178**, 625–646 (2008).
13. Esleta, G. A. & Monterola, C. Effect of memory and reinforcement on the propagation and morphology of fracture in a two-dimensional mass-spring system. *Int'l. J. of Modern Phys. C* **20**, 1049–1062 (2009).
14. Albert, R. & Barabasi, A. L. Statistical mechanics of complex networks. *Rev. Mod. Phys.* **74**, 47–97 (2002).
15. Kun, F., Carmona, H. A. & Herrmann, H. J. Universality behind Basquin's law of fatigue. *Phys. Rev. Let.* **100**, 094301 (2008).
16. Barabási, A. L. Scale-free networks: a decade and beyond. *Science* **325**, 412–413 (2009).
17. Barabási, A. L., Jeong, H., Néda, Z. Ravasz, E. Schubert, A. & Vicsek, T. Evolution of the social network of scientific collaborations. *Physica A* **311**, 590–614 (2002).
18. Barabási, A. L., Albert, R. & Jeong, H. Scale-free characteristics of random networks: the topology of the world-wide web. *Physica A* **281**, 69–77 (2000).

Acknowledgments

Author contributions

Conceived and designed the experiment: C.M. and C.A. Performed the numerical experiments: C.A. Analyzed the data: C.A., C.M. and E.F.L. Wrote the paper: C.A., C.M. and E.F.L. All authors reviewed the manuscript.

Additional information